Scientific Research Publishing

Journal of Biosciences and Medicines, 2025, 13(7), 90-104
https://www.scirp.org/journal/jbm
ISSN Online: 2327-509X
ISSN Print: 2327-5081

Comparative Bioinformatics Analysis of Ewing's Sarcoma and Femoral Head Necrosis

Yanlin He[1,2,3], Fengqing Liao[1,2,3], Jialong Huang[1,2,3], Junxiu Zhou[4], Mingxuan Liu[1,2,3], Jiahou Xu[1,2,3], Huang Wen[1,2,3], Yongfu Chen[1,2,3], Pengyuan He[1,2,3], Huan Zhang[1,2*]

[1]Affiliated Hospital of Youjiang Medical University for Nationalities, Baise, China
[2]Biomedical Materials Engineering Research Center for Bone and Joint Degenerative Diseases, Guangxi Zhuang Autonomous Region, Baise, China
[3]Graduate School, Youjiang Medical University for Nationalities, Baise, China
[4]Department of Pharmacy, Baise Maternal and Child Health Hospital, Baise, China
Email: *2598540061@qq.com

How to cite this paper: He, Y.L., Liao, F.Q., Huang, J.L., Zhou, J.X., Liu, M.X., Xu, J.H., Wen, H., Chen, Y.F., He, P.Y. and Zhang, H. (2025) Comparative Bioinformatics Analysis of Ewing's Sarcoma and Femoral Head Necrosis. *Journal of Biosciences and Medicines*, **13**, 90-104.
https://doi.org/10.4236/jbm.2025.137007

Received: May 17, 2025
Accepted: July 11, 2025
Published: July 14, 2025

Abstract

Objective: To screen and analyze the differentially expressed genes (DEGs) in Ewing's sarcoma (ES) and osteonecrosis of the femoral head (ONFH) using bioinformatics. **Methods**: Using the GEO gene chip public database in NCBI for data retrieval, select chip data GSE17674 and GSE74089 as analysis objects. Using the R language limma toolkit to screen for DEmRNAs, and standardizing the data, a Venn diagram was used to screen for common differentially expressed genes between the two; perform GO functional and KEGG pathway enrichment analysis on common differentially expressed genes using the R language clusterProfiler package. Select String database for PPI analysis, import the results into Cytoscape software to obtain PPI mapping, core modules, and Hub genes. Download the known genes of ES and ONFH from the OMIM database, intersect them with the core module genes screened by MOCDE, and obtain the COL11A1 gene; intersect the genes downloaded from the OMIM database with the screened differentially expressed genes to obtain four genes: COL11A1, KIT, KRAS, and MSH2. Then intersect the genes obtained from both to obtain the COL11A1 gene. **Conclusion:** The differentially expressed genes and related signaling pathways identified can help understand the molecular mechanisms underlying the pathogenesis of ES and ONFH, providing a basis for early diagnosis of ES combined with ONFH; the drug prediction results can provide second-line drugs for the clinical treatment of ES combined with ONFH, and provide new ideas for clinical drug treatment research.

*Corresponding author.

Keywords

ES, ONFH, Bioinformatics Analysis, Differentially Expressed Gene, Signal Pathway

1. Background

Osteonecrosis of the femoral head (ONFH) is a common progressive disease in orthopedics, often resulting in femoral head ischemia due to bone ischemia, osteocyte necrosis and other factors. These lead to subsequent cascade reactions that ultimately lead to femoral head necrosis and collapse [1]. This condition results in a high disability rate and a heavy medical burden. Approximately 8.12 million people suffer from this disease in China. Of the 200,000 hip replacements performed annually in the United States, 10% to 15% have ONFH. In Northern Europe and Russia, ONFH accounts for 30% of orthopedic diseases [2]. ONFH is a disease caused by multiple factors, and its pathogenesis can involve impaired blood supply, endothelial injury, genetic susceptibility, abnormal apoptosis of bone cells, abnormal lipid metabolism, osteoporosis, oxidative stress, long-term chronic inflammation, intraosseous high pressure, thrombosis and coagulation disorders [1] [3]-[5].

Ewing's sarcoma (ES) is the second most common bone tumor and the commonest osteosarcoma in children and adolescents. ES is a malignant bone tumor characterized by low differentiation, high invasiveness, a high local recurrence rate and distant metastasis [6] [7]. Studies have found that ES most frequently occurs in the tubular bones of the limbs (46%), followed by the pelvis (22%), ribs and spine [8] [9]. ES mutations include chromosomal translocations between members of the EWSR1 and ETS (E26 transformation-specific) transcription factor families. The most common are FLI1 (t(11; 22)(q24; q12)) and EWSR1-FLI1 reprogram epigenetic states and changes in gene expression, thus leading to tumorigenesis [10].

ES presents with extensive osteolytic destruction and mass-occupying lesions, leading to bone pain and pathological fracture. However, ES does not directly damage bone tissue, but the release of osteoclast activating factors (such as IL-6 and TNF-α) as well as chemotactic inflammatory cells, which activate the inflammatory response. These will lead to an immune and osteoclast imbalance. Bone destruction is greater than its formation as the activated osteoclasts absorb bone tissue. The release of growth factors from the bone matrix (including IGF-1, FGFs and TGF-β) activates tumor cell proliferation, which is the "vicious cycle" associated with ES [11]-[13]. This "vicious cycle" can lead to an imbalance in skeletal dynamics, which often causes complications such as femoral head necrosis, osteoporosis and brittle fracture in ES patients. Therefore, ES can be a risk factor for the onset of ONFH, but the question as to whether there is a gene-level correlation between the two conditions remains unclear.

We conducted bioinformatics analysis on ES and ONFH data obtained from the Gene Expression Omnibus (GEO) and the gene chip data of the control population, and studied the key genes and their molecular networks. We explored the possible molecular biological functions involved. This study provides a theoretical basis for revealing the potential correlation and molecular mechanism of the two conditions.

2. Methods

2.1. Data Collection

We searched using the keywords "Ewing's Sarcoma" and "Necrosis of Femoral Head" in the public gene expression omnibus (GEO) database of the U.S. National Center for Biotechnology Information. We obtained the original data of the ES patient data chip GSE17674 and ONFH patient data chip GSE74089. GSE17674 included 44 patients with ES and 18 patients without ES. The GSE74089 chip dataset had 4 patients with MFH and 4 patients without ONFH. We then used the R language limma package to screen of the differentially expressed genes (DEGs) from ES and OP mRNA chip data with P values < 0.05 and a fold change (FC) of logarithm absolute value |log FC| > 2 as the filter. This identified the differentially expressed mRNAs (DEmRNAs) between the two datasets. The common target genes at the intersection of ES and ONFH gene data were obtained.

2.2. GO Function and KEGG Signal Pathway Enrichment Analysis

The R clusterProfiler package was used for GO and KEGG enrichment analysis and the GO functions of the two generic DEmRNAs were enriched to analyze the biological processes associated. The KEGG signaling pathways were enriched simultaneously.

2.3. PPI and Core Module Analysis

The interacting genes were analyzed by the online STRING (search tool for the retrieval of interacting genes/proteins) 11.0 tool. Cytoscape 3.9.1 software was imported into the STRING calculation results. Cytohubba, CytoNCA and MCODE were used as Cytoscape 3.9.1 protein interaction network maps to co-express the core genes and modules.

2.4. Screening of Core Genes Related to Both

We searched the Online Catalog of Human Genes and Genetic Diseases (OMIM, https://omim.org/) with the keywords "Ewing's sarcoma" and "Necrosis of ONFH" in//omim.org/, and searched for the genes related to ES and ONFH diseases reported in the literature. We then used a Venn diagram to show the intersected genes with the key protein molecules obtained through MCODE analysis.

2.5. KEGG and GSEA Pathway Enrichment Analyses

The core DEGs in the chip dataset were screened using gene set enrichment anal-

ysis (GSEA), and the KEGG gene set was used as the preset gene set for this in order to select the key genes involved. The candidate genes related to ES and ONFH reported in the OMIM database were also intersected by using a Venn diagram for GSEA pathway enrichment analysis.

2.6. Hub Gene Localization

Tissue localization of the hub gene was conducted by the online database BioGPS (http://biogps.org/#goto=welcome). The highest inter-tissue expression level was significantly greater and twice the second highest expression level, indicating that this gene could be used as a marker gene of ES and ONFH common expression.

3. Results

3.1. Identification of Comorbidity mRNAs

The R language limma package was used to analyze the differential expression of gene chips for the two diseases. We found that the expression levels of most genes were consistent, indicating that the data were suitable for further analysis (Figure 1).

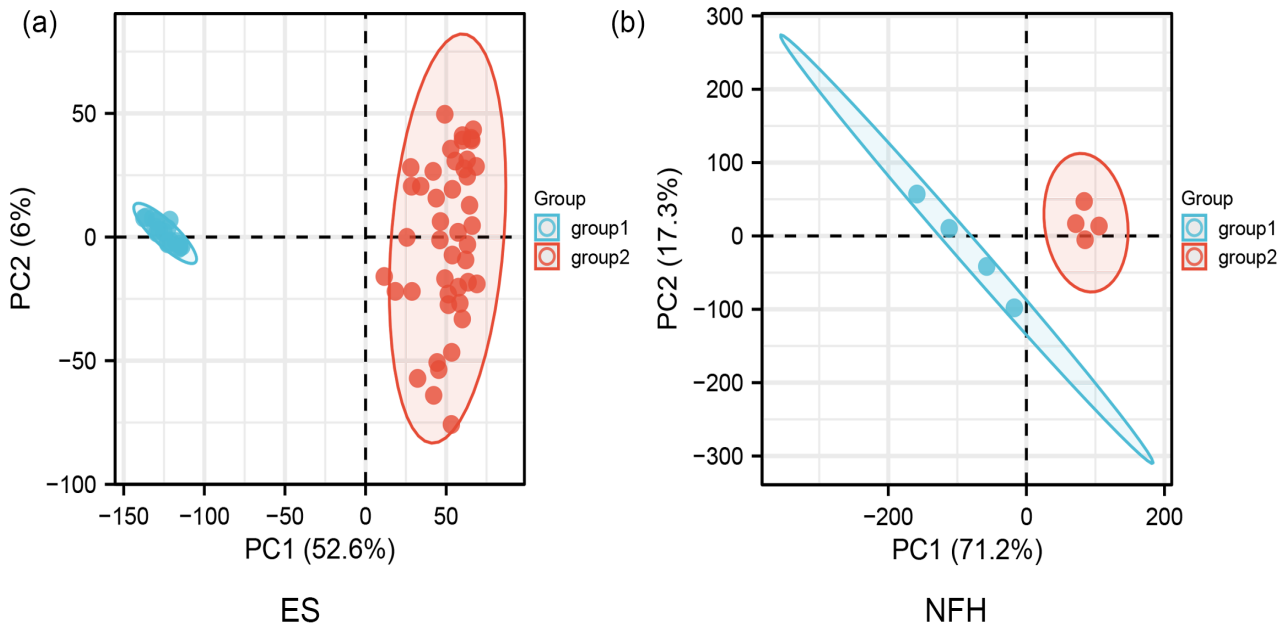

Note: (a) is the GSE17674 data chip box diagram, and (b) is the GSE74089 data chip box diagram.

Figure 1. Boxplot of gene expression.

1817 and 1787 DEGs were identified between ES and ONFH patients and healthy individuals, respectively (Figure 2). In addition, when the intersection of these two datasets was determined, 668 genes were found to be co-expressed (Figure 3).

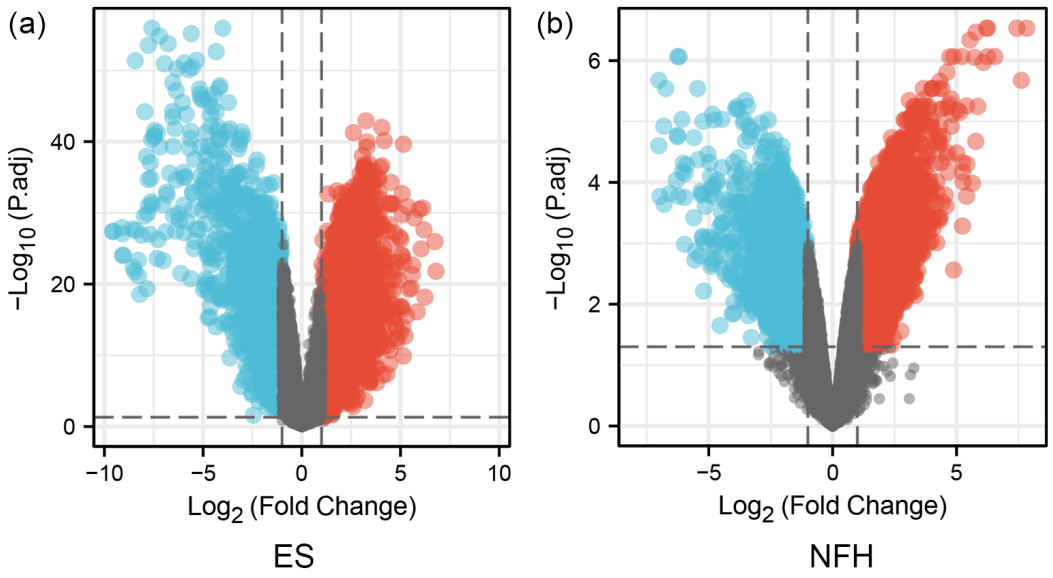

Note: (a) represents the volcano map of the GSE17674 dataset, (b) represents the volcano map of the GSE35958 dataset; blue and red represent downregulated and upregulated genes, respectively.

Figure 2. A Volcano map of the results obtained.

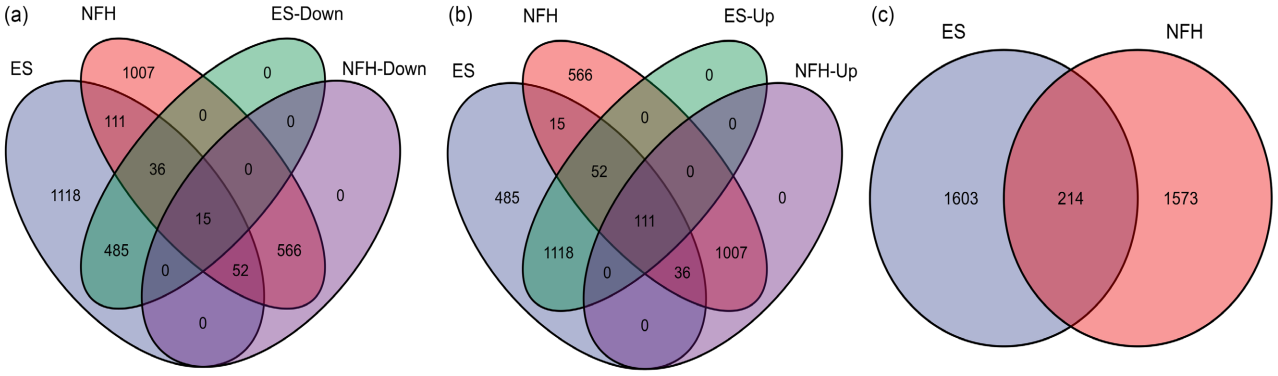

Note: (a) represents the upregulated genes Venn diagram, (b) represents the downregulated genes and (c) represents the co-expressed genes.

Figure 3. A Venn diagram of the ES and ONFH intersecting genes in this study.

3.2. GO and KEGG Enrichment Analysis of Intersected Genes

The GO and KEGG pathways of ES and ONFH were enriched by the R clusterProfiler package. The signaling pathways involved in biological processes (BP), cellular components (CC) and molecular functions (MF) as well as KEGG were analyzed. BP mainly showed enrichment in extracellular structure organization, ossification and extracellular matrix organization (**Figure 4(a)**; **Table 1**). CC and MF were mainly enriched in collagen-containing extracellular matrix and collagen trimer (**Figure 4(b)**; **Table 2**) and in the extracellular matrix structural, actin binding and actin filament binding (**Figure 4(c)**; **Table 3**). The KEGG pathways were mainly concentrated in focal adhesion kinase and proteoglycans involved in the cancer signaling pathways (**Figure 4(d)**; **Table 4**).

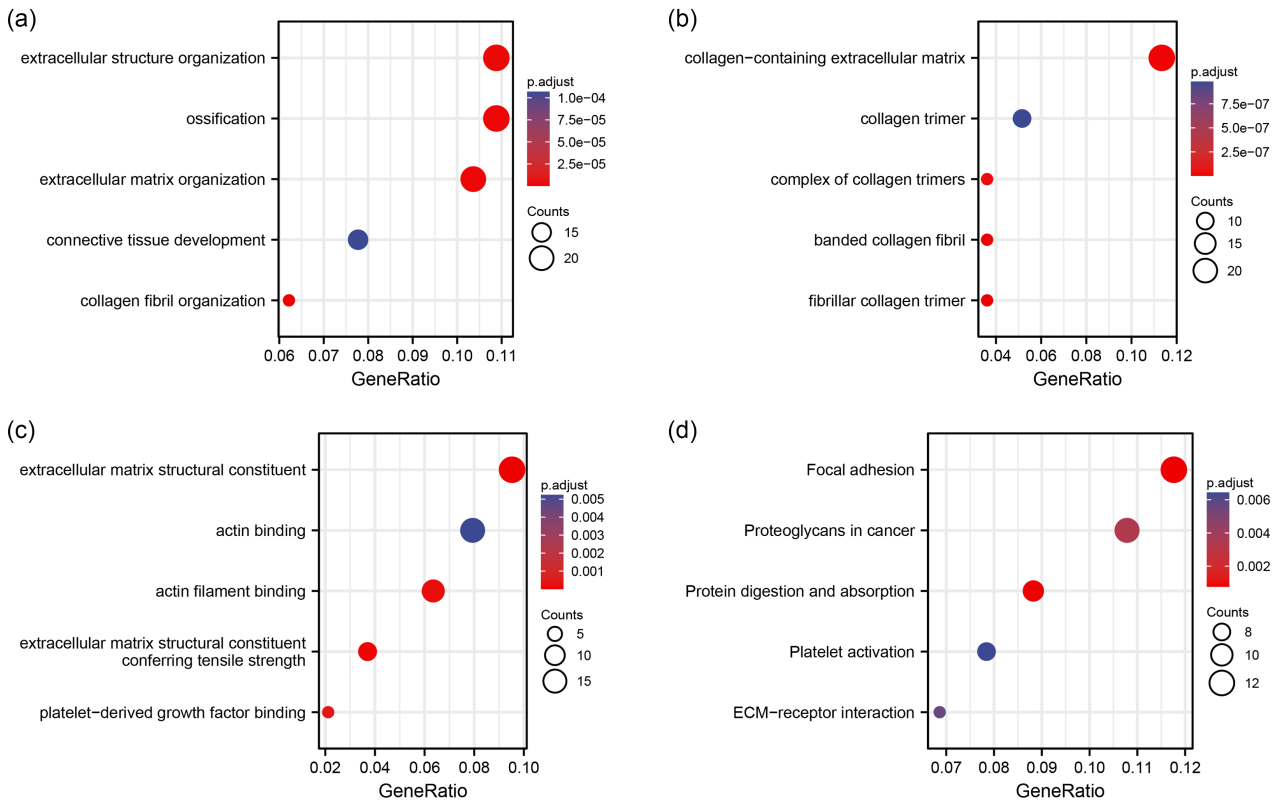

Note: (a): BP, (b): CC, (c): MF, (d): KEGG.

Figure 4. GO functional enrichment and KEGG pathway analyses.

Table 1. The results of GO biological process analysis.

ID	Description	P value	Count
GO:0030198	Extracellular matrix organization	<0.01	76
GO:0043062	Extracellular structure organization	<0.01	83
GO:0031647	Regulation of protein stability	<0.01	62
GO:0031589	cell-substrate Adhesion	<0.01	72
GO:0051169	Nuclear transport	<0.01	70
GO:0060348	Bone development	<0.01	50
GO:0001503	Ossification	<0.01	77
GO:0006913	nucleocytoplasmic Transport	<0.01	69
GO:0008380	RNA splicing	<0.01	86
GO:0034504	Protein localization to nucleus	<0.01	56

Table 2. The results of GO cell component analysis.

ID	Description	P value	Count
GO:0005925	Focal adhesion	<0.01	95
GO:0005924	cell-substrate Adherens junction	<0.01	95
GO:0030055	Cell-substrate junction	<0.01	95

Continued

GO:0005635	Nuclear envelope	<0.01	95
GO:0062023	Collagen-containing extracellular matrix	<0.01	84
GO:0031252	Cell leading edge	<0.01	82
GO:0016607	Nuclear speck	<0.01	75
GO:0031965	Nuclear membrane	<0.01	58
GO:0035770	Ribonucleoprotein granule	<0.01	46
GO:0030027	Lamellipodium	<0.01	41

Table 3. The results of GO molecular function analysis.

ID	Description	P value	Count
GO:0005201	Extracellular matrix structural constituent	<0.01	44
GO:0050839	Cell adhesion molecule binding	<0.01	91
GO:0003725	Double-stranded RNA binding	<0.01	23
GO:0005518	Collagen binding	<0.01	20
GO:0017124	SH3 domain binding	<0.01	31
GO:0004842	Ubiquitin-protein transferase activity	<0.01	68
GO:0019787	Ubiquitin-like protein transferase activity	<0.01	71
GO:0045182	Translation regulator activity	<0.01	18
GO:0043394	Proteoglycan binding	<0.01	13
GO:0005200	Structural constituent of cytoskeleton	<0.01	25

Table 4. The results of KEGG analysis.

ID	Description	P value	Count
hsa05205	Proteoglycans in cancer	<0.01	44
hsa03018	RNA degradation	<0.01	22
hsa04510	Focal adhesion	<0.01	42
hsa05100	Bacterial invasion of epithelial cells	<0.01	20
hsa05132	*Salmonella* infection	<0.01	46
hsa04512	ECM-receptor interaction	<0.01	21
hsa04810	Regulation of actin cytoskeleton	<0.01	41
hsa00510	N-Glycan biosynthesis	<0.01	14
hsa05130	Pathogenic *Escherichia coli* infection	<0.01	37
hsa03013	RNA transport	<0.01	35

3.3. Construction of a PPI Network and Prediction of Core Genes

The STRING online tool was used to analyze 214 common DEmRNAs. The minimum interaction score was set as 0.4, and an interaction diagram consisting of 2146 nodes and 2928 lines was obtained. These results were imported into Cytoscape 3.9.1 software to obtain the PPI interaction network. The genes with highest betweenness centrality (BC) were arranged clockwise based on their scores after

processing by using the BC algorithm of the CytoNCA plug-in (Figure 4(a)). The generic expression gene modules were obtained by using the MOCDE algorithm in the Cytoscape plug-in, and we obtained 7 core modules with scores greater than 4 (Figure 4(b), Figure 4(c), Figure 4(d)). Ten hub genes were obtained by using 10 different nodal centrality algorithms, including maximal clique centrality (MCC), density of maximum neighbourhood component (DMNC) and maximum neighborhood component (MNC), in the cytoHubba plugin (Figure 5). These genes were COL1A1, COL1A2, COL3A1, FN1, COL5A2, COL5A1, POSTN, LUM, COL6A2 and LOX in that order based on the scores obtained.

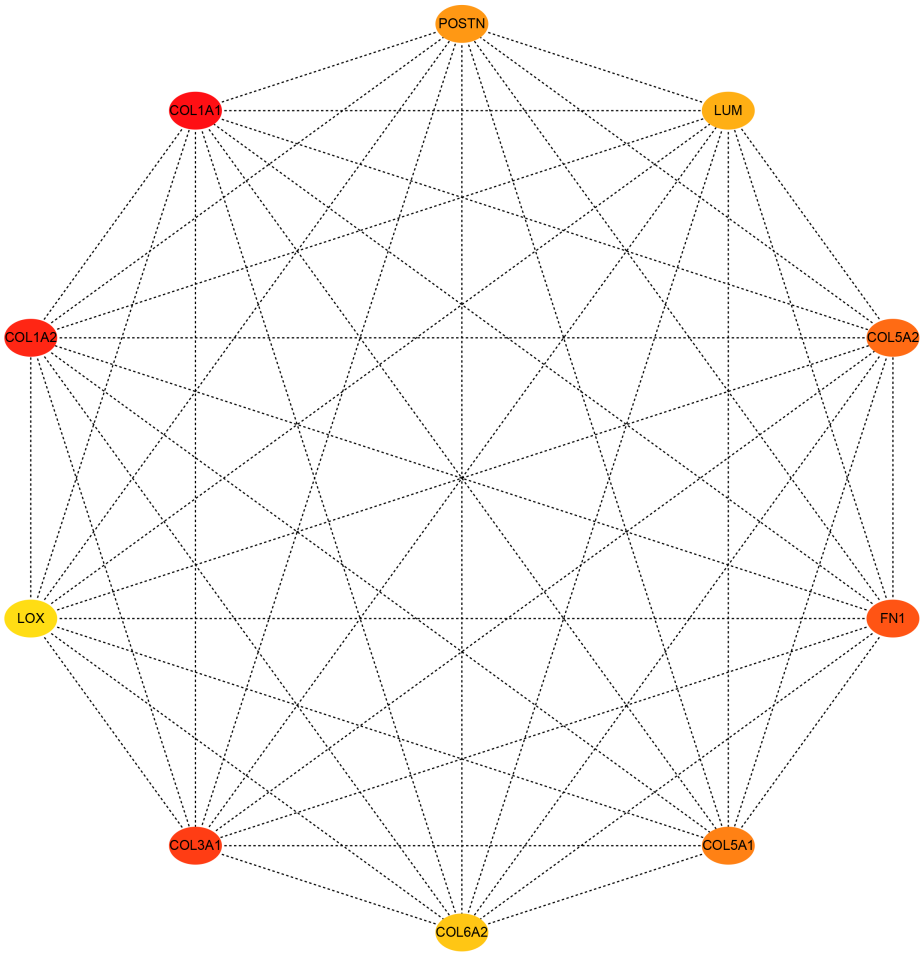

Note: Red indicates a higher enrichment score, the lighter color indicates a lower score, and the connection lines indicate the interaction between the genes.

Figure 5. The core module of the hub genes.

3.4. Core Genes

The genes related to ES and ONFH reported in the literature were searched in the OMIM online catalog of human genes and genetic diseases, and the duplicate genes were removed. Finally, 1025 genes related to ES and ONFH were obtained. The intersection of the above genes and 33 key protein molecules obtained from

MCODE analysis was assessed in a Venn diagram (Figure 6(a)), and a candidate gene, COL11A1, was obtained.

3.5. GSEA of DEGs

GSEA gene set enrichment analysis was conducted using KEGG gene sets as the preset gene sets to analyze the chip data sets. With a P value < 0.05 as the screening criterion for enrichment pathways related to ES and ONFH traits, 29 KEGG pathways were obtained in the GSE17674 chip and 11 KEGG pathways in the GSE74089 chip. The core genes in these enriched pathways were intersected with the disease-related genes of the two obtained from the OMIM database. Four genes (Figure 6(b)) were found to be common in the two gene sets and OMIM, namely COL11A1, KIT, KRAS, andMSH2 (GSEA was generated by Xiantao Academic Online and the parameters have been set).

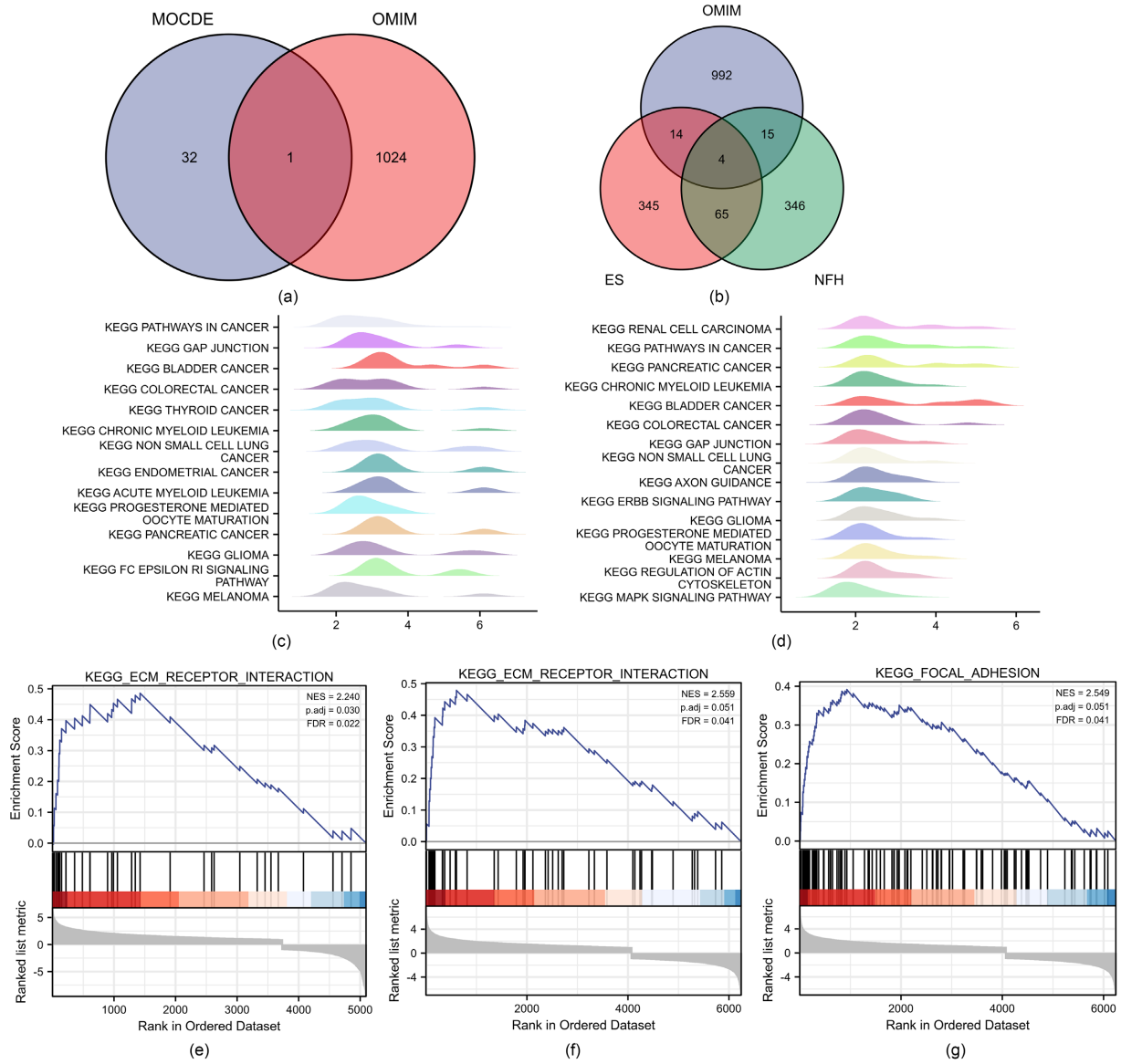

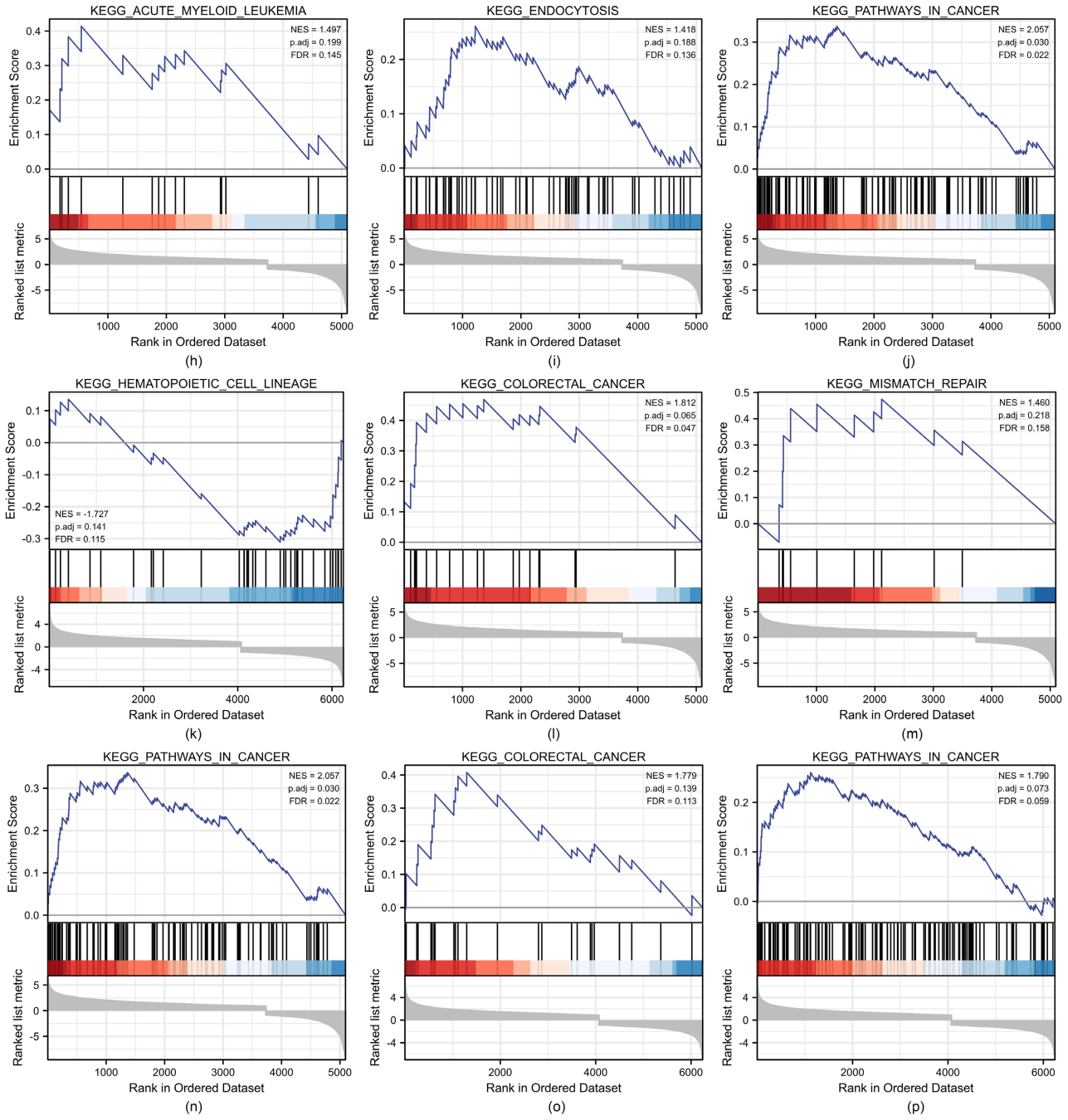

Note: (a) is the intersecting gene of the MCODE module and OMIM; (b) is the intersecting gene of GSEA and OMIM for ES and ONFH; (c) and (d) are enrichment analyses of the KRAS pathway of the KRAS gene; (e), (f), and (g) are enrichment analyses of the GSEA pathway of the COL11A1 gene. (h), (i), (j), and (k) are enrichment analyses of the KIT gene pathway. (l), (m), (n), (o), (p) are MSH2 gene pathway enrichment analyses.

Figure 6. The core genes and GSEA.

In the GSE17674 chip, KRAS is related to pathways in cancer, gap junction, bladder cancer, colorectal cancer, thyroid cancer, chronic myeloid leukemia (CML), non-small cell lung cancer (NSCLC), endometrial cancer, acute ML (AML), progesterone-mediated oocyte maturation, pancreatic cancer, glioma, Fc epsilon RI sig-

naling pathway and the melanoma pathway (**Figure 6(c)**, **Figure 6(d)**). COL11A1 is a core gene involved in ECM receptor interactions and pathways (**Figure 6(e)**). KIT is a core gene involved in endocytosis, pathways in cancer and AML (**Figure 6(h)**, **Figure 6(i)**, **Figure 6(j)**). MSH2 is a core gene in pathways in cancer, colorectal cancer (CRC) and mismatch repair (**Figure 6(l)**, **Figure 6(m)** and **Figure 6(n)**).

COL11A1 is a core gene involved in the focal adhesion and ECM receptor interaction pathway in the GSE74089 dataset (**Figure 6(f)** and **Figure 6(g)**). KRAS is involved in renal cell carcinoma, pathways in cancer, pancreatic cancer, CML, bladder cancer, CRC, gap junction, non-small lung cancer, axon guidance, Erbb signaling pathway, glioma, progesterone-mediated oocyte core genes of maturation, melanoma, regulation of actin cytoskeleton and the MAPK signaling pathways (**Figure 6(b)**). KIT is a core gene involved in the hematopoietic cell lineage pathway (**Figure 6(k)**). MSH2 is a core gene in pathways in cancer and CRC (**Figure 6(o)** and **Figure 6(p)**).

3.6. Final Gene Screening

After analysis, it was found that the common gene among OMIM, MCODE, and GSEA is COL11A1.

4. Discussion

We screened for genes related to ES and ONFH that have been reported in the literature using the OMIM Human Gene and Genetic Disease Database. Finally, we intersected the differentially expressed genes and core modules with the reported genes in the OMIM library using Venn diagrams, and obtained the COL11A1 core gene.

COL11A1 is a core gene in the ECM receptor interaction pathway, KRAS is a core gene in chronic myeloid leukemia and other pathways, KIT is a core gene in endocytosis, cancer, and acute myeloid leukemia pathways, MSH2 is a core gene in cancer and heterologous repair pathways. These signaling pathways and diseases are closely related to the pathogenesis of ES and ONFH, and COL11A1 can serve as an independent marker gene for ES combined with ONFH. Therefore, the diagnosis and treatment of ES combined with ONFH in the long term can be based on basic research on COL11A1.

ONFH is associated with microcirculatory disruption caused by multiple factors, including alcohol consumption, chemotherapy, immune disorders, chronic inflammation, leukemia, sickle cell disease, HIV infection, bone tumors, etc., all of which can lead to microcirculatory obstruction of the femoral head and are independent risk factors for ONFH [4] [14] [15]. With the development of medical technology, surgical, chemotherapy, radiotherapy and other methods can effectively treat primary tumors, but the efficacy for patients with metastasis and recurrence is poor, and the long-term survival rate (OS) of ES is less than 30%; The use of angiogenesis inhibitors in solid tumor patients can significantly improve the prognosis of ES patients [16]. Vascular endothelial growth factor (VEGF)

plays an important role in promoting ES angiogenesis, and tumor cells produce one or more VEGF subtypes that stimulate the proliferation and survival of related tumor endothelial cells through their receptors VEGFR-1 and VEGFR-2 [17]. Endothelial cells in ES exhibit a high proliferation rate, and like most tumors, the average serum VEGF level in ES patients is higher than that in healthy controls [18]. In response, anti-tumor angiogenesis and vascular targeted therapy have been proposed, and bevacizumab is a monoclonal antibody targeting all human VEGF subtypes [19]. Preliminary clinical efficacy analysis found that bevacizumab has a significant effect in inhibiting ES growth [20]. However, long-term use of such targeted drugs can affect the formation of normal bone tissue blood vessels in the body, causing heterogeneous and disordered blood flow in tumor blood vessels, reducing efficacy, and accompanied by serious side effects, resulting in complications such as abnormal blood supply to the femoral head and femoral head necrosis [21]. Chemotherapy and radiotherapy can significantly alter the physiological functions of cells and tissues, leading to endocrine disorders, hormonal metabolism disorders, accelerated cell aging, gene mutations, and accumulation of reactive oxygen species (ROS), all of which are initiating factors leading to chronic inflammation; The body is in a chronic inflammatory state for a long time, and inflammatory factors such as IL-6 and TNF-α are gradually activated, leading to unstable bone metabolism balance and increased risk of bone loss and infarction, which is consistent with the pathogenesis of ONFH [22]. The above results indicate that ES may be an independent risk factor for femoral head necrosis, suggesting that the two may be causally related, but the specific molecular mechanism is still unclear.

The COL11A1 gene encodes the type XI collagen alpha 1 chain and is a member of the collagen family. Type XI collagen is mainly distributed in cartilage and connective tissue, and its core function is to participate in the assembly and structural maintenance of collagen fibers, especially in the interaction with type II collagen in the cartilage matrix, regulating fiber diameter and network stability. 1) The mechanical properties of extracellular matrix (ECM) are crucial for the development and repair of bones and joints. 2) Mutation can lead to genetic diseases (such as Sticker syndrome, Marshall syndrome), manifested as abnormal cartilage development, skeletal deformities, etc.

Ewing's sarcoma is a malignant tumor originating from bone or soft tissue, and its pathological mechanism is related to COL11A1 in the following aspects: abnormal gene expression and tumor microenvironment: 1) COL11A1 is highly expressed in Ewing's sarcoma: Studies have found that Ewing's sarcoma cells can abnormally synthesize type XI collagen, promoting ECM remodeling in the tumor microenvironment. 2) Potential interaction with EWSR1 gene: The characteristic fusion gene EWSR1-FLI1 in Ewing's sarcoma can regulate the expression of ECM related genes (including COL11A1), forming a matrix environment that promotes tumor growth. 3) The abnormal deposition of type XI collagen may alter the mechanical signaling of tumor cells, activate proliferative pathways such as PI3K/AKT, and enhance cell survival ability. In animal models, inhibiting COL11A1 expres-

sion can reduce lung metastasis of Ewing's sarcoma, suggesting that it may become a potential therapeutic target [23] [24].

The core pathology of femoral head necrosis is ischemic death of bone cells and destruction of bone matrix. The role of COL11A1 involves genetic susceptibility and imbalance of matrix homeostasis: 1) COL11A1 mutations and abnormal bone development: missense mutations of COL11A1 (such as glycine substitution) have been detected in some cases of familial femoral head necrosis, leading to abnormal structure of type XI collagen and affecting the mechanical strength of subchondral bone. 2) Association with Sticker syndrome: This syndrome is caused by COL11A1 mutation, and patients often have hip dysplasia, which can progress to femoral head necrosis in the later stage, suggesting that COL11A1 functional defects can increase the risk of disease through abnormal bone development. 3) Type XI collagen is an important component of the subchondral bone cartilage interface, and its abnormalities can lead to: imbalanced mineralization of the bone matrix, increasing the risk of microfractures; Obstruction of angiogenesis affects the repair of femoral head blood supply and exacerbates ischemic injury. In the hormone induced femoral head necrosis model, downregulation of COL11A1 expression can lead to disordered arrangement of subchondral collagen fibers and reduced bone stress resistance [25] [26].

In this study, GO, KEGG and KEGG enrichment analyses of DEGs showed that these were mainly enriched in muscle structure development and actin cytoskeleton tissue and they were related to the striated muscle contraction pathway and RUNX3 regulation of CDKN1A transcription. As a therapeutic target for ES, EWS/FLI has only been found to be expressed in ES at present. RUNX protein is closely related to the Runt domain of EWS/FLI. RUNX1 and RUNX3, which are subtypes of RUNX, can promote the occurrence of various tumors, and RUNX3 can be detected in all ES tumors [23]. The signaling pathways associated with RUNX3 regulation of CDKN1A transcription may provide a direction for further research on the related immune system factors associated with ES.

5. Summary and Outlook

All of these genes are involved to varying degrees in the occurrence and development of ES and ONFH, and many of these are related to inflammation and immune dysfunction. This provides new ideas for further research on the role and correlation of the immune system in the pathogenesis of these two conditions.

Data Availability

All data included or relevant to the study are available upon request by contacting the corresponding author.

Conflicts of Interest

All the authors declare that they have no commercial or associative interest that represents competing interests in connection with the work submitted.

References

[1] Wang, P., Wang, C., Meng, H., Liu, G., Li, H., Gao, J., *et al.* (2022) The Role of Structural Deterioration and Biomechanical Changes of the Necrotic Lesion in Collapse Mechanism of Osteonecrosis of the Femoral Head. *Orthopaedic Surgery*, **14**, 831-839. https://doi.org/10.1111/os.13277

[2] Zhao, D., Zhang, F., Wang, B., Liu, B., Li, L., Kim, S., *et al.* (2020) Guidelines for Clinical Diagnosis and Treatment of Osteonecrosis of the Femoral Head in Adults (2019 Version). *Journal of Orthopaedic Translation*, **21**, 100-110. https://doi.org/10.1016/j.jot.2019.12.004

[3] Jilka, R.L., Noble, B. and Weinstein, R.S. (2013) Osteocyte apoptosis. *Bone*, **54**, 264-271. https://doi.org/10.1016/j.bone.2012.11.038

[4] Hines, J.T., Jo, W., Cui, Q., Mont, M.A., Koo, K., Cheng, E.Y., *et al.* (2021) Osteonecrosis of the Femoral Head: An Updated Review of ARCO on Pathogenesis, Staging and Treatment. *Journal of Korean Medical Science*, **36**, e177. https://doi.org/10.3346/jkms.2021.36.e177

[5] An, F., Zhang, L., Gao, H., Wang, J., Liu, C., Tian, Y., *et al.* (2020) Variants in RETN Gene Are Associated with Steroid-Induced Osteonecrosis of the Femoral Head Risk among Han Chinese People. *Journal of Orthopaedic Surgery and Research*, **15**, Article No. 96. https://doi.org/10.1186/s13018-020-1557-3

[6] Gurung, S., Thapa, S. and Gautam, S. (2022) Extraosseous Ewing Sarcoma in a Pelvic Region: A Case Report. *Journal of Nepal Medical Association*, **60**, 638-640. https://doi.org/10.31729/jnma.7523

[7] Twardziok, M., Kleinsimon, S., Rolff, J., Jäger, S., Eggert, A., Seifert, G., *et al.* (2016) Multiple Active Compounds from Viscum Album L. Synergistically Converge to Promote Apoptosis in Ewing Sarcoma. *PLOS ONE*, **11**, e0159749. https://doi.org/10.1371/journal.pone.0159749

[8] Jiang, Y., Zhao, L., Wang, Y., Liu, X., Wu, X. and Li, Y. (2020) Primary Intracranial Ewing Sarcoma/Peripheral Primitive Neuroectodermal Tumor Mimicking Meningioma: A Case Report and Literature Review. *Frontiers in Oncology*, **10**, Article 528073. https://doi.org/10.3389/fonc.2020.528073

[9] Li, W., Dong, S., Lin, Y., Wu, H., Chen, M., Qin, C., *et al.* (2022) A Tool for Predicting Overall Survival in Patients with Ewing Sarcoma: A Multicenter Retrospective Study. *BMC Cancer*, **22**, Article No. 914. https://doi.org/10.1186/s12885-022-09796-7

[10] Li, M. and Chen, C. (2022) Epigenetic and Transcriptional Signaling in Ewing Sarcoma—Disease Etiology and Therapeutic Opportunities. *Biomedicines*, **10**, Article 1325. https://doi.org/10.3390/biomedicines10061325

[11] Lau, Y.S., Adamopoulos, I.E., Sabokbar, A., Giele, H., Gibbons, C.L.M.H. and Athanasou, N.A. (2007) Cellular and Humoral Mechanisms of Osteoclast Formation in Ewing's Sarcoma. *British Journal of Cancer*, **96**, 1716-1722. https://doi.org/10.1038/sj.bjc.6603774

[12] Redini, F. and Heymann, D. (2015) Bone Tumor Environment as a Potential Therapeutic Target in Ewing Sarcoma. *Frontiers in Oncology*, **5**, Article 279. https://doi.org/10.3389/fonc.2015.00279

[13] Ma, J., Ge, J., Gao, F., Wang, B., Yue, D., Sun, W., *et al.* (2019) The Role of Immune Regulatory Cells in Nontraumatic Osteonecrosis of the Femoral Head: A Retrospective Clinical Study. *BioMed Research International*, **2019**, Article ID: 1302015. https://doi.org/10.1155/2019/1302015

[14] Mont, M.A., Salem, H.S., Piuzzi, N.S., Goodman, S.B. and Jones, L.C. (2020) Non-

traumatic Osteonecrosis of the Femoral Head: Where Do We Stand Today? *Journal of Bone and Joint Surgery*, **102**, 1084-1099. https://doi.org/10.2106/jbjs.19.01271

[15] Dzik-Jurasz, A.S.K., Brooker, S., Husband, J.E. and Tait, D. (2001) What Is the Prevalence of Symptomatic or Asymptomatic Femoral Head Osteonecrosis in Patients Previously Treated with Chemoradiation? A Magnetic Resonance Study of Anal Cancer Patients. *Clinical Oncology*, **13**, 130-134. https://doi.org/10.1053/clon.2001.9236

[16] DuBois, S.G., Marina, N. and Glade-Bender, J. (2009) Angiogenesis and Vascular Targeting in Ewing Sarcoma: A Review of Preclinical and Clinical Data. *Cancer*, **116**, 749-757. https://doi.org/10.1002/cncr.24844

[17] Li, T., Kang, G., Wang, T. and Huang, H. (2018) Tumor Angiogenesis and Anti-angiogenic Gene Therapy for Cancer (Review). *Oncology Letters*, **16**, 687-702. https://doi.org/10.3892/ol.2018.8733

[18] Fuchs, B., Inwards, C.Y. and Janknecht, R. (2004) Vascular Endothelial Growth Factor Expression Is Up-Regulated by EWS-ETS Oncoproteins and Sp1 and May Represent an Independent Predictor of Survival in Ewing's Sarcoma. *Clinical Cancer Research*, **10**, 1344-1353. https://doi.org/10.1158/1078-0432.ccr-03-0038

[19] Zhou, Z., Bolontrade, M.F., Reddy, K., Duan, X., Guan, H., Yu, L., *et al.* (2007) Suppression of Ewing's Sarcoma Tumor Growth, Tumor Vessel Formation, and Vasculogenesis Following Anti-Vascular Endothelial Growth Factor Receptor-2 Therapy. *Clinical Cancer Research*, **13**, 4867-4873. https://doi.org/10.1158/1078-0432.ccr-07-0133

[20] Bender, J.L.G., Adamson, P.C., Reid, J.M., Xu, L., Baruchel, S., Shaked, Y., *et al.* (2008) Phase I Trial and Pharmacokinetic Study of Bevacizumab in Pediatric Patients with Refractory Solid Tumors: A Children's Oncology Group Study. *Journal of Clinical Oncology*, **26**, 399-405. https://doi.org/10.1200/jco.2007.11.9230

[21] Morrell, M.B.G., Alvarez-Florez, C., Zhang, A., Kleinerman, E.S., Savage, H., Marmonti, E., *et al.* (2019) Vascular Modulation through Exercise Improves Chemotherapy Efficacy in Ewing Sarcoma. *Pediatric Blood & Cancer*, **66**, e27835. https://doi.org/10.1002/pbc.27835

[22] Rossi, F., Tortora, C., Paoletta, M., Marrapodi, M.M., Argenziano, M., Di Paola, A., *et al.* (2022) Osteoporosis in Childhood Cancer Survivors: Physiopathology, Prevention, Therapy and Future Perspectives. *Cancers*, **14**, Article 4349. https://doi.org/10.3390/cancers14184349

[23] Zhang, J., Lu, S., Lu, T., Han, D., Zhang, K., Gan, L., *et al.* (2023) Single-Cell Analysis Reveals the COL11A1^{+} Fibroblasts Are Cancer-Specific Fibroblasts That Promote Tumor Progression. *Frontiers in Pharmacology*, **14**, Article 1121586. https://doi.org/10.3389/fphar.2023.1121586

[24] Hassan, M., Yasir, M., Shahzadi, S. and Kloczkowski, A. (2022) Exploration of Potential Ewing Sarcoma Drugs from FDA-Approved Pharmaceuticals through Computational Drug Repositioning, Pharmacogenomics, Molecular Docking, and MD Simulation Studies. *ACS Omega*, **7**, 19243-19260. https://doi.org/10.1021/acsomega.2c00518

[25] Hao, Y., Lu, C., Zhang, B., Xu, Z., Guo, H. and Zhang, G. (2021) Identifying the Potential Differentially Expressed miRNAs and mRNAs in Osteonecrosis of the Femoral Head Based on Integrated Analysis. *Clinical Interventions in Aging*, **16**, 187-202. https://doi.org/10.2147/cia.s289479

[26] Liu, Y., Ma, Y., Yang, W., Lin, Q., Xing, Y., Shao, H., *et al.* (2024) Integrated Proteomics and Metabolomics Analysis of Sclerosis-Related Proteins and Femoral Head Necrosis Following Internal Fixation of Femoral Neck Fractures. *Scientific Reports*, **14**, Article No. 13207. https://doi.org/10.1038/s41598-024-63837-8